

# Compression with Global Guidance: Towards Training-free High-Resolution MLLMs Acceleration

Xuyang Liu, Ziming Wang, Yuhang Han, Yingyao Wang, Jiale Yuan, Jun Song, Bo Zheng, Linfeng Zhang, Siteng Huang, and Honggang Chen, *Member, IEEE*

**Abstract**—Multimodal large language models (MLLMs) have attracted considerable attention due to their exceptional performance in visual content understanding and reasoning. However, their inference efficiency has been a notable concern, as the increasing length of multimodal contexts leads to quadratic complexity. Token compression techniques, which reduce the number of visual tokens, have demonstrated their effectiveness in reducing computational costs. Yet, these approaches have struggled to keep pace with the rapid advancements in MLLMs, especially the AnyRes strategy in the context of high-resolution image understanding. In this paper, we propose a novel token compression method, GlobalCom<sup>2</sup>, tailored for high-resolution MLLMs that receive both the thumbnail and multiple crops. GlobalCom<sup>2</sup> treats the tokens derived from the thumbnail as the “commander” of the entire token compression process, directing the allocation of retention ratios and the specific compression for each crop. In this way, redundant tokens are eliminated while important local details are adaptively preserved to the highest extent feasible. Empirical results across 10 benchmarks reveal that GlobalCom<sup>2</sup> achieves an optimal balance between performance and efficiency, and consistently outperforms state-of-the-art token compression methods with LLaVA-NeXT-7B/13B models. Our code is released at <https://github.com/xuyang-liu16/GlobalCom2>.

**Index Terms**—Multi-modal large language models, token compression, vision and language, efficient inference.

## I. INTRODUCTION

**B**Y bridging a visual encoder with the pre-trained Large Language Model (LLM) [1]–[3] decoder, Multimodal

This work was supported in part by the National Natural Science Foundation of China (Grant Nos. 62001316), in part by Sichuan Science and Technology Program under Grant 2024YFHZ0212, in part by the Open Foundation of Yunnan Key Laboratory of Software Engineering under Grant 2023SE206, and in part by the Fundamental Research Funds for the Central Universities under Grant SCU2023D062 and under Grant 2022CDSN-15-SCU. (*Corresponding author: Honggang Chen and Jun Song.*)

Xuyang Liu is with the College of Electronics and Information Engineering, Sichuan University, Chengdu 610065, China (email: liuxuyang@stu.scu.edu.cn).

Ziming Wang, Yingyao Wang, Jiale Yuan, Jun Song, and Bo Zheng are with the Taobao & Tmall Group of Alibaba, Beijing 100102, China (email: {shaoqing.wzm, wangyingyao.wyy, yuanjiale.yjl, jsong.sj, bozheng}@alibaba-inc.com).

Yuhang Han is with the College of Aulin, Northeast Forestry University, Harbin 150040, China (email: hanyh@nefu.edu.cn).

Linfeng Zhang is with the School of Artificial Intelligence, Shanghai Jiao Tong University, Shanghai 200030, China (email: zhanglinfeng@sjtu.edu.cn).

Siteng Huang is with the College of Computer Science and Technology, Zhejiang University, Hangzhou 310007, China (email: siteng.huang@gmail.com).

Honggang Chen is with the College of Electronics and Information Engineering, Sichuan University, Chengdu 610065, China, and also with the Yunnan Key Laboratory of Software Engineering, Yunnan University, Kunming 650600, China (e-mail: honggang\_chen@scu.edu.cn).

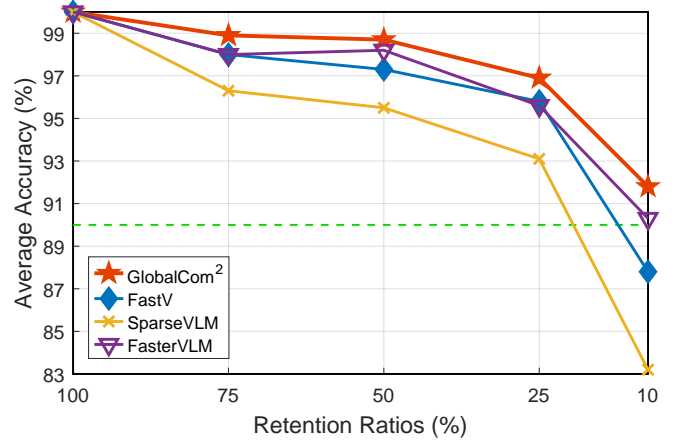


Fig. 1. Average accuracy comparisons of our GlobalCom<sup>2</sup> with other training-free MLLM token compression methods on LLaVA-NeXT-7B across 10 benchmarks. GlobalCom<sup>2</sup> achieves over 90% average accuracy (green dashed line) while retaining only 10% of visual tokens.

Large Language Models (MLLMs) [4]–[7] have achieved remarkable progress in handling various vision-language tasks. This integration allows MLLMs to understand both visual and textual data to perform complex tasks such as visual question answering [8], image captioning [9], referring expression comprehension [10], and multimodal reasoning [11]. However, the extracted visual features, when integrated with textual instructions, increase the length of the input. And a quadratic complexity scaled with context length results in prohibitive computational and memory demands, limiting the practical deployment of MLLMs in real-world settings.

To tackle the challenge of inference speed in MLLMs, researchers have turned their attention to developing acceleration techniques for MLLMs, which has become a critical demand for both academia and industry. The majority of these acceleration strategies are model-centric, encompassing approaches such as knowledge distillation [12] and model quantization [13]. However, these solutions typically necessitate retraining, which incurs additional computational costs. Furthermore, they are frequently designed for specific network architectures or rely heavily on empirical techniques, limiting their practical applicability and broad utility. Recent efforts, exemplified by token compression methods [14]–[18], have shifted their focus towards enhancing inference speed by minimizing data redundancy. These methods aim to reduce the amount of tokens that need to be processed while preserving the essential information required for the model to make accurate predictions. Their architecture-agnostic characteristic allows

for their application across MLLMs with diverse structures. Additionally, when retraining is not available, training-free token compression methods can still achieve an optimal balance between efficiency and accuracy [19]–[21].

However, current token compression methods are only suitable for traditional MLLMs. As technology progresses, the demand for interpreting high-resolution images has become more pressing. Traditional MLLMs, with their standard architecture, often fail to capture the full range of details within images. Consequently, LLaVA-NeXT [22] and InternVL 1.5 [23] have introduced a cropping-based approach known as AnyRes, which divides a high-resolution image into several sub-images (*i.e.*, crops), each encoded individually and then concatenated with tokens from the resized original image (*i.e.*, thumbnail). This enables LLMs to receive a greater number of visual tokens at various scales, allowing them to focus on more image details for a comprehensive understanding of image content and precise command execution. However, AnyRes also increases the number of visual tokens and further reduces the inference speed of MLLMs. Directly applying existing token compression methods to all views, including the thumbnail and all the crops, might seem like a straightforward solution to mitigate the overhead introduced by AnyRes. Yet, this approach not only overlooks the varying contributions of the thumbnail and crops to visual content expression, but also compresses each crop from a limited local perspective. This can lead to the loss of important local details during compression, which finally results in suboptimal accuracy.

In this paper, we perform systematic experiments and analysis to examine the roles of global thumbnails and local crops in high-resolution MLLM image understanding capabilities. Through our empirical investigation, we identify **two key insights**: (1) Visual tokens from global thumbnails and local crops serve complementary purposes, where thumbnail tokens capture holistic context while local crop tokens preserve fine-grained visual details. (2) Visual tokens from different local crops exhibit varying levels of semantic richness and redundancy, which directly impacts their contributions to high-resolution MLLM image understanding.

Building on these insights, we propose an effective token compression method **GlobalCom<sup>2</sup>** (short for “**Global Compression Commander**”), specifically designed for high-resolution MLLMs. Our method follows a “**global-to-local**” design philosophy and operates in two stages. In the first stage, GlobalCom<sup>2</sup> leverages thumbnail information to evaluate the semantic significance of each local crop, enabling adaptive token retention rates across different regions. In the second stage, it performs token compression on both the thumbnail and local crops, where the compression of local crops is guided by thumbnail information to maximize the preservation of crucial visual details. Through this hierarchical approach, GlobalCom<sup>2</sup> achieves efficient and adaptive token compression while maintaining essential visual information.

To evaluate the effectiveness and efficiency of the proposed method, we conduct extensive experiments across 10 multimodal understanding benchmarks. As shown in Figure 1, our GlobalCom<sup>2</sup> consistently outperforms existing training-free methods across various retention ratios. In particular, even in

the extreme case where 90% of visual tokens are pruned, our method can still sustain over 90% of the original performance. Furthermore, in tasks that demand a deeper understanding of local details, such as text recognition and multimodal hallucination evaluation, our experimental findings indicate that GlobalCom<sup>2</sup> holds a significant advantage over other baselines. We attribute this to the capability of our method to adaptively preserve more critical local information based on global context.

The remainder of this paper is organized as follows. In Section II, we briefly review the related work on conventional MLLMs, high-resolution MLLMs, and token compression methods. We then provide a detailed description of our proposed method and its core designs, followed by a discussion of theoretical complexity analysis in Section III. In Section IV, we present extensive quantitative and qualitative experiments to analyze the performance and efficiency of the proposed method. Finally, we summarize our work in Section V.

## II. RELATED WORK

### A. Multimodal Large Language Models (MLLMs)

To develop visual comprehension and reasoning skills, MLLMs [4], [6], [24], [25] generally integrate a pre-trained vision encoder for extracting visual features and a pre-trained LLM decoder for generating text sequences. To bridge the two parts, a visual projector is employed to map the visual features into the input embedding space of the LLM decoder, thereby creating a multimodal prompt that incorporates user instructions. For instance, BLIP-2 [24] utilizes a frozen Flan-T5 model for multimodal understanding and trains a Q-Former as the visual projector to bridge the modality gap. LLaVA [4] fine-tunes a simple linear projector and LLM with a high-quality visual instruction tuning dataset in a two-stage process, which promotes alignment between vision and language spaces. Building on this, LLaVA-1.5 [5] replaces the linear projector with a multi-layer perceptron (MLP) to further refine the integration of visual and textual information.

### B. High-resolution MLLMs

To maintain consistency with the image resolution employed during pre-training, MLLMs typically resize images to a predefined resolution before feature extraction. However, this strategy often results in significant shape distortion and blurring. Moreover, when processing high-resolution images, this simply resizing can lead to excessive loss of local details, thereby causing recognition errors or hallucinations. To address this, the AnyRes practice, introduced in LLaVA-NeXT [22] and InternVL 1.5 [23], segments high-resolution images into multiple regions, each processed independently and then concatenated with visual tokens from the original image’s thumbnail. The AnyRes strategy has been adopted in subsequent works [26]–[28] to accommodate higher resolutions. Particularly, augmenting the number of local visual tokens aids the model in discerning local details, and significantly enhances performance in scenarios requiring text recognition or hallucination suppression. However, while improving the understanding of high-resolution images, more crops also introduce a larger number of visual tokens, potentially making

inference speed and memory usage the limiting factors for MLLMs in practical applications.

### C. Token Compression

Token compression approaches can be broadly categorized into two dominant techniques. While token pruning [29], [30] directly eliminates less important tokens, token merging [31]–[33] attempts to compress tokens into a smaller set of more compact units, predicated on the assumption that such a strategy minimizes information loss. While earlier studies have predominantly concentrated on ViTs, recent efforts focus on accelerating the inference of MLLM. For example, FastV [20] prunes unnecessary visual tokens based on the ranking of attention scores derived from the self-attention mechanism in the LLM. SparseVLM [19] adaptively prunes visual tokens in the LLM based on their attention scores with text tokens. FasterVLM [21] utilizes [CLS] attention scores from the visual encoder to re-rank visual tokens and retains the top ones. However, they are not specially designed for high-resolution MLLMs, making them sub-optimal when applying to high-resolution MLLMs. In this paper, we design a training-free method for off-the-shelf high-resolution MLLMs equipped with the AnyRes strategy.

## III. METHODOLOGY

In this section, we present our GlobalCom<sup>2</sup> in detail. First, we briefly revisit LLaVA-NeXT, a representative high-resolution MLLM, in Section III-A. Through systematic analytical experiments, we identify fundamental insights into the characteristics of high-resolution MLLMs and, based on these insights, present the detailed design of our training-free method GlobalCom<sup>2</sup> in Section III-B. Finally, we provide an in-depth analysis of theoretical complexity in Section III-C.

### A. Preliminary: LLaVA-NeXT

In this work, we employ LLaVA-NeXT [22], a widely-adopted high-resolution MLLM, to demonstrate the effectiveness of our proposed training-free token compression strategy.

*a) Model Architecture:* Building on the findings from LLaVA-NeXT, enhancing input image resolution can boost the capabilities of LLMs compared to the models limited to fixed-resolution images. Following this work, we implement high-resolution vision encoding and language model instruction following through these three module designs:

- **Vision Encoder:** Same configuration as LLaVA-NeXT model, CLIP-ViT-L-336px is used for visual encoding, transforming raw pixels into unified image space representation.
- **Projector:** A two-layer MLP is employed to project visual embeddings into the word embedding space in the vision-language connector module.
- **LLM:** The decoder-only model structure using the next token prediction paradigm has better zero-shot generalization performance on downstream tasks. By concatenating image tokens derived from the vision encoder with text tokens comprised of the system prompt and user prompt, which are then used as input for the LLMs, the LLM Decoder would generate the final response.

*b) AnyRes Input Pre-processing:* Enhancing input image resolution while maintaining the original aspect ratio greatly supports the model’s fine-grained semantic comprehension. Due to the fixed resolution of CLIP vision encoder used by most MLLMs, the size of all input images is limited to 336x336 pixels. Previous approaches typically employ positional embedding interpolation and adapt ViT backbone to the new fixed size resolution by finetuned on a large-scale visual-text dataset, yet they still fall short of adapting to the original image size during inference [5], [6], [24].

LLaVA-NeXT utilizes adaptive dynamic cropping to accommodate images of any resolution. Specifically, we define a series of grid configurations:  $\{2 \times 2, 1 \times \{2, 3, 4\}, \{2, 3, 4\} \times 1\}$ , resulting in seven cropping templates. Within the constraints of the ViT’s fixed size, LLaVA-NeXT achieves a maximum resolution of  $672 \times 672$  pixels.

Assuming in a vision encoder, each image is assigned a visual token length  $N$  and the fixed resolution of visual encoder is  $w \times h$ . For an input image width  $W$ , height  $H$ , the image is scaled to  $(w \times a) \times (h \times b)$ , employing padding strategy to preserve the original aspect ratio of image as much as possible. We utilize two routes to process the image: first, by dividing it into  $a \times b$  local crops, denoted as  $\mathbf{X}^L$ , and second, by keeping a resized version as a global thumbnail, denoted as  $\mathbf{X}^G$ . The total visual tokens of  $\mathbf{X}^G$  and  $\mathbf{X}^L$  is  $T = (1 + a \times b) \times N$ .

*c) Visual Tokens Post-processing:* Edge padding strategy used in image cropping preserves the original aspect ratio while introducing extra pixels, leading to visual noise and reducing token utilization efficiency when the sequence is compressed. Therefore, during the visual token post-processing stage, following [5], LLaVA-NeXT implements an unpadding strategy where features corresponding to padding tokens are discarded, and a special token is appended to the end of each feature row to explicitly indicate the image shape.

This strategy elegantly preserves the original image size information while eliminating redundant representations, thus reducing the visual token sequence length and substantially improving both training and inference efficiency.

### B. Global Compression Commander: GlobalCom<sup>2</sup>

The AnyRes strategy adopted by high-resolution MLLMs enables LLMs to capture high-resolution visual signals with richer details, however, it introduces substantially more visual tokens. Taking LLaVA-NeXT [22] as an example, its AnyRes strategy extends the length of visual tokens to approximately **3-5 times** more than before, significantly increasing the computational complexity and consequently reducing the inference speed for LLMs. Specifically, the computational complexity of self-attention [34] scales **quadratically** with sequence length, which poses a significant challenge as the increasing length of multi-modal contexts results in prohibitive computational and memory demands, limiting the practical applications of high-resolution MLLMs.

Based on the above analysis, we aim to enhance the inference efficiency of high-resolution MLLMs by directly reducing the computational costs through visual token sequence compression (*i.e.*, token compression). Given that LLaVA-NeXT partitions

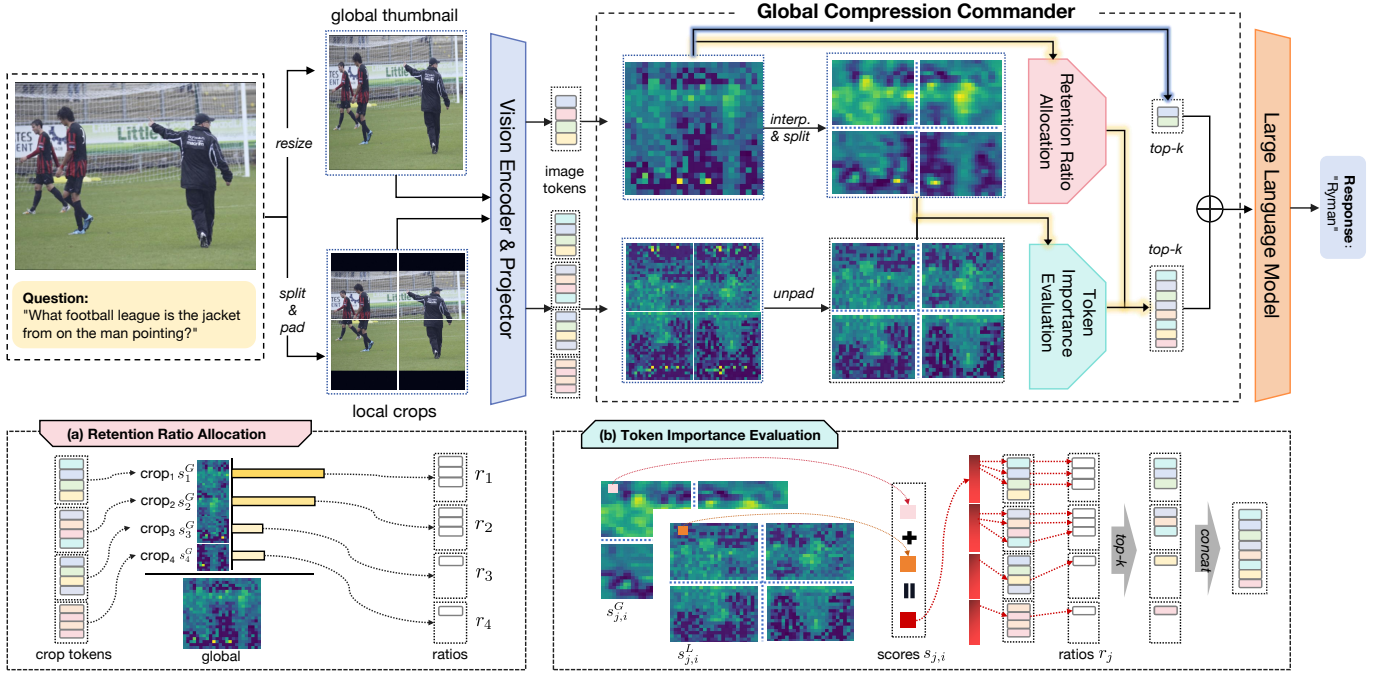


Fig. 2. **Overall framework of GlobalCom<sup>2</sup>.** GlobalCom<sup>2</sup> guides token compression for high-resolution MLLMs through: 1) compressing global thumbnail tokens (blue shaded path); 2) compressing local crop tokens (yellow shaded paths) by: (a) allocating optimal retention ratios based on each crop’s importance to the global image, and (b) performing token compression by jointly considering token importance at both global and local levels.

TABLE I  
PERFORMANCE ANALYSIS OF LLaVA-NeXT UNDER DIFFERENT IMAGE INPUTS ACROSS VARIOUS BENCHMARKS.

Method	VQA <sup>T</sup>	POPE	SQA	MMB	MM-Vet
LLaVA-NeXT-7B	61.3	86.5	70.1	67.4	43.9
<i>(a) Effects of Global Thumbnail and Local Crops</i>					
Global thumbnail only	56.8	84.6	<b>70.9</b>	<b>67.3</b>	<b>42.4</b>
Local crops only	<b>57.5</b>	<b>87.3</b>	68.0	65.0	40.8
<i>(b) Effects of Different Local Crops</i>					
Random crop removal	56.4	86.1	66.9	64.7	36.6
Important crop removal	54.3	85.3	65.3	65.4	36.1
Unimportant crop removal	<b>57.5</b>	<b>87.0</b>	<b>68.4</b>	<b>66.3</b>	<b>38.5</b>

input images into a global thumbnail followed by a series of local crops as shown in the top-left of Figure 2, performing visual token compression for LLaVA-NeXT involves compressing tokens from both the global thumbnail and local crops.

We begin with an exploratory experiment to investigate how global thumbnails and local crops differently contribute to image understanding in high-resolution MLLMs by using them separately as input to LLaVA-NeXT. As shown in Table I (a), using global thumbnail alone yields superior performance on general visual perception benchmarks such as SQA [35], MMB [36], and MM-Vet [37]. This advantage stems from global thumbnails serving as *comprehensive visual extractor*, providing holistic visual information through complete ViT encoding. In contrast, using only local crops, where ViT independently encodes each crop, shows inferior performance on these general visual perception tasks due to the lack of holistic visual information. However, local crops excel in fine-grained perception tasks like VQA<sup>T</sup> (requiring text recognition

in images) and POPE (testing model hallucination), as they provide more detailed visual features. Therefore, we argue that **1) global thumbnails and local crops play distinct roles in visual perception tasks of high-resolution MLLMs**, thus requiring different token compression strategies.

Furthermore, given the global thumbnail’s capability as a *comprehensive visual extractor* that captures the entire input image’s visual information from a holistic perspective, we propose to leverage it as a “**Global Compression Commander**” (GlobalCom<sup>2</sup>) to guide token compression for high-resolution MLLMs, as shown in Figure 2. In what follows, we will elaborate on how our GlobalCom<sup>2</sup> guides token compression for both the global thumbnail and local crops.

*a) Global Thumbnail Compression:* The core principle of visual token compression should be to preserve important tokens while reducing less significant ones. For the global thumbnail, which needs to provide LLMs with holistic visual information, important visual tokens are naturally those that can best summarize the overall image information. Previous works [18], [31] have consistently found that the [CLS] token in ViT effectively represents global image representation.

Based on this insight, as shown in the blue shaded path in Figure 2, GlobalCom<sup>2</sup> leverages the attention map from the last ViT layer to compute the average attention value between each global thumbnail token and the [CLS] token across all attention heads. This last layer attention map contains the richest semantic information for measuring token importance [21]. Specifically, for 1D token sequence  $\mathbf{X}^G$  of length  $N$  in the global thumbnail, the importance score  $s_i^G$  for the  $i$ -th token can be written as:

$$s_i^G = \frac{\exp(\mathbf{q}^{\text{CLS}} \mathbf{K}_i^{\text{T}} / \sqrt{D})}{\sum_{i=1}^N \exp(\mathbf{q}^{\text{CLS}} \mathbf{K}_i^{\text{T}} / \sqrt{D})}, \quad (1)$$

where  $\mathbf{q}^{\text{CLS}}$  is the query projection of the [CLS] token,  $\mathbf{K} \in \mathbb{R}^{N \times D}$  are obtained by projecting  $\mathbf{X}^G$  with learnable parameter matrices,  $^\top$  denotes the transpose of the matrix. Therefore, visual tokens with higher  $s^G$  contain richer semantic information and highlight globally important visual features, thus should be preserved. Conversely, tokens with lower  $s^G$  are directly dropped from  $\mathbf{X}^G$ . We preset a token retention ratio  $R$  for GlobalCom<sup>2</sup>, which preserves the top- $k$  ( $k = R \times N$ ) visual tokens based on their  $s^G$  to reduce the visual token sequence length for the global thumbnail.

To this end, GlobalCom<sup>2</sup> achieves training-free token compression for the global thumbnail by preserving tokens with high semantic importance while compressing less significant ones, based on each visual token’s semantic significance in the global thumbnail. This global compression mechanism of GlobalCom<sup>2</sup> reduces the computational cost of high-resolution MLLMs for global thumbnail processing, thereby partially accelerating model inference.

*b) Local Crop Compression:* Due to the AnyRes strategy’s image partitioning, local crops produce longer visual token sequences with more redundancy compared to the global thumbnail. Furthermore, each local crop contains distinct visual information, leading to varying amounts of informational content across crops. As shown in Figure 2, the upper two crops contain significant entity information, such as football players, while the lower two crops exhibit considerable visual redundancy, predominantly showing large areas of grass. The visualization in the upper middle of Figure 2 displays the attention values between tokens in the global thumbnail and the [CLS] token, clearly demonstrates higher attention values in the upper regions, indicating that the upper two local crops contain richer semantic information from a global perspective.

Moreover, based on our previous analysis, the attention scores with the [CLS] token effectively measure the semantic information contained in a token. Therefore, we partition the 2D attention map of the global thumbnail according to the crop segmentation pattern, and sum up the scores in each sub-attention map to obtain the global importance of that crop. We investigate the varying contributions of different local crops to image understanding in high-resolution MLLMs by selectively dropping local crops from the input image sequence of LLaVA-NeXT (randomly dropping one crop, dropping the most important crop, and dropping the least important crop, respectively). As demonstrated in Table I (b), different local crops contribute differently to visual understanding due to their varying semantic richness. Specifically, when dropping the most important versus the least important crops, we observe significant performance gaps across various visual understanding tasks, particularly in VQA<sup>T</sup> for text recognition, where the gap reaches 3.2. This indicates that different crops contribute varying degrees of detail comprehension, while also suggesting that semantically richer local crops are more crucial for fine-grained visual understanding.

Based on the above qualitative and quantitative analysis, we argue that ② *each local crop contributes differently to the overall visual understanding of high-resolution MLLMs*, thus warranting varying degrees of token compression.

Local crops containing rich semantic information in the

context of the entire image should retain more visual tokens, providing LLMs with semantically dense visual information to capture crucial local visual details. Conversely, crops with limited semantic content should undergo more aggressive token compression, allowing LLMs to focus on semantically rich visual signals. Based on the above analysis and motivated by observations ①-②, we aim to guide the token compression of local crops from a global perspective. Specifically, GlobalCom<sup>2</sup> incorporates *two aspects of global guidance* for local crop token compression: retention ratio allocation and token importance evaluation.

• **Retention Ratio Allocation.** As presented in the bottom-left of Figure 2, GlobalCom<sup>2</sup> first analyzes the semantic contribution of each local crop to the overall visual information, adaptively allocating appropriate retention ratios based on their contribution levels.

Specifically, for the  $j$ -th local crop, GlobalCom<sup>2</sup> compute its cumulative [CLS] attention score over its corresponding region in the global thumbnail, denoted as  $s_j^G$ :

$$s_j^G = \sum_{m \in \text{crop}_j} s_m^G, \quad (2)$$

where  $s_m^G$  represents the individual scores of tokens within the crop over its corresponding region in the global thumbnail. The shifted score  $\tilde{s}_j$  is then calculated by normalizing  $s_j^G$  with the maximum score  $\max(s_j^G)$ :

$$\tilde{s}_j = \frac{s_j^G - \max(s_j^G)}{\tau}, \quad (3)$$

where  $\tau$  is the temperature hyper-parameter used for scaling, with a default value of 10. Subsequently, the relative weights  $\sigma_j$  are computed using the softmax function:

$$\sigma_j = \frac{\exp(\tilde{s}_j)}{\sum_{l=1}^n \exp(\tilde{s}_l) + 1 \times 10^{-8}}, \quad (4)$$

where a small constant  $10^{-8}$  is added to prevent division by zero. The weights  $\sigma_j$  indicate the level of contribution toward the initial retention ratio  $r'_j$ :

$$r'_j = R \times \left( 1 + \sigma_j - \frac{1}{n} \sum_{l=1}^n \sigma_l \right), \quad (5)$$

where  $R$  is the pre-set base retention ratio. Finally, the  $j$ -th crop’s retention ratio  $r_j$  is adjusted to ensure it does not exceed 1.0, expressed as:

$$r_j = \min(r'_j, 1.0). \quad (6)$$

Through above careful design, our GlobalCom<sup>2</sup> is capable of allocating optimal retention ratios to each local crop based on their representations of global visual information, thereby commanding high-resolution MLLMs to perform differentiated token compression across local crops.

• **Token Importance Evaluation.** After obtaining the optimal retention ratio for each local crop, GlobalCom<sup>2</sup> further evaluates the importance of tokens within each crop and preserves the essential visual tokens, as shown in the bottom-right of Figure 2. After independent ViT encoding of each local crop, we obtain attention values between each token and the [CLS]

token, reflecting each token’s representational capacity for global information within the crop.

Similar to token importance evaluation in the global thumbnail, GlobalCom<sup>2</sup> leverages the attention map between tokens and the [CLS] token from the final ViT layer to assign a local importance score  $s_{j,i}^L$  to the  $i$ -th token in the  $j$ -th crop, reflecting its significance within its corresponding crop. Here,  $s^L$  represents the attention scores after removing padding tokens from local crops, effectively capturing the semantic information of actual image content. However, since local crops are encoded independently,  $s^L$  is only able to measure token importance within its respective crop, without reflecting its significance in the context of the complete image.

Given this limitation, GlobalCom<sup>2</sup> aims to capture both the token’s importance within its local crop and its significance in the global context, enabling token compression in local crops to be guided by both local and global perspectives, thereby preserving more essential and informative local details. Specifically, as shown in Figure 2, GlobalCom<sup>2</sup> first reshapes the 1D attention scores  $s^G$  between tokens and the [CLS] token from the global thumbnail into a 2D format, and then resizes it to match the original high-resolution image dimensions through bilinear interpolation (refer to "interp." in Figure 2). Subsequently, the interpolated attention map is split into multiple sub-attention maps according to the local crop partitioning, where these sub-attention maps are able to measure the semantic significance of tokens in local crops from a global perspective. By combining these sub-attention maps with the attention maps from individual local crops, we can comprehensively evaluate token importance from both global and local perspectives.

Specifically, the comprehensive importance score  $s_{j,i}$  for the  $i$ -th token in the  $j$ -th local crop is calculated by integrating its global score  $s_{j,i}^G$  from the global sub-attention map and its local score  $s_{j,i}^L$  from the local crop’s attention map with [CLS] token, formulated as:

$$s_{j,i} = \alpha s_{j,i}^G + (1 - \alpha) s_{j,i}^L \quad (7)$$

Here,  $\alpha$  serves as a scalar hyper-parameter to balance the contributions of two importance scores, with a default value of 0.5 to equally weight both importance scores. Subsequently, for the  $j$ -th crop, according to the retention ratio  $r_j$  allocated by our GlobalCom<sup>2</sup>, we retain the top- $k$  visual tokens, where  $k = r_j \times N$ , based on their comprehensive importance scores  $s^j$  to compress the visual tokens in  $j$ -th crop. To this end, our GlobalCom<sup>2</sup> adaptively preserves tokens in local crops that are globally significant while containing rich local details, offering fine-grained visual insights for LLM.

### C. Discussion: Theoretical Complexity Analysis

GlobalCom<sup>2</sup> compresses a large number of visual tokens for high-resolution MLLMs, thereby reducing their computational costs. Below, we analyze the theoretical computational complexity of high-resolution MLLMs in both the prefill stage and the decoding stage.

During the prefill stage, the FLOPs for a single transformer layer can be estimated using the formula  $8Td^2 + 4T^2d + 6Tdm$ .

When applying a token retention ratio  $R$ , where the retained token count is defined as  $\hat{N} = R \cdot N$ , the corresponding theoretical FLOPs reduction ratio  $\eta$  can be reformulated to account for this adjustment:

$$\begin{aligned} \eta &= 1 - \frac{8\hat{T}d^2 + 4\hat{T}^2d + 6\hat{T}dm}{8Td^2 + 4T^2d + 6Tdm} \\ &= 1 - \frac{R(8d + 4RTd + 6m)}{8d + 4Td + 6m} \end{aligned} \quad (8)$$

In the decoding stage, the integration of a KV-Cache substantially enhances computational efficiency. This improvement is evidenced by the reduction in the complexity of attention computation to  $\mathcal{O}(T)$ . As a result, the formula for computing FLOPs is refined to  $8d^2 + 4Td + 6Tdm$ . Given the current limitations of hardware, managing dynamic KV-Cache lengths effectively during the inference process presents significant challenges. Therefore, implementing pruning strategies prior to the decoder in large language models could facilitate a more efficient acceleration of the inference process.

## IV. EXPERIMENTS

In this section, we first introduce the experimental settings, including benchmark descriptions, implementation details, and baseline methods in Section IV-A. Then, we provide comprehensive comparisons and analysis across 10 benchmarks in Section IV-B. In Section IV-C, we conduct detailed ablation studies to analyze the designs of our GlobalCom<sup>2</sup>, followed by thorough efficiency analysis. Finally, in Section IV-D, we present multiple visualization results to provide insights into the compression performance of our GlobalCom<sup>2</sup>.

### A. Experimental Setting

a) *Benchmark Details*: To evaluate the effectiveness and efficiency of our GlobalCom<sup>2</sup>, we conducted comprehensive experiments across 10 widely used multimodal understanding benchmarks, consisting of 5 academic task-oriented benchmarks and 5 instruction-following benchmarks.

**Academic-task-oriented Benchmarks.** We conduct evaluations of our GlobalCom<sup>2</sup> on VQAv2 [38], GQA [39], VizWiz [40], ScienceQA (SQA) [35], and TextVQA (VQA<sup>T</sup>) [41]. VQAv2 [38] and GQA [39] are fundamental visual reasoning benchmarks, with VQAv2 containing 265,016 real-world images and crowd-sourced questions, while GQA uses scene graphs for structured reasoning. VizWiz [40] features 31,000 visual questions from blind users with lower quality images and a conversational style. SQA [35] tests scientific reasoning in 26 topics and 379 skills, while VQA<sup>T</sup> [41] evaluates the comprehension of text embedded in images.

**Instruction-following Benchmarks.** We also conduct our GlobalCom<sup>2</sup> on POPE [42], MME [43], MMBench (MMB) [36], MMBench-CN (MMBCN) [36] and MM-Vet [37]. POPE [42] focuses on detecting object hallucination through binary questions, employing multiple metrics and sampling strategies for precise evaluation. MME [43] assesses 14 perceptual and cognitive subtasks using carefully designed instruction-answer pairs. MMB [36] tests for robustness by re-shuffling

TABLE II

COMPARISON WITH OTHER TRAINING-FREE MLLM TOKEN COMPRESSION METHODS WITH LLaVA-NeXT-7B ACROSS 10 BENCHMARKS. “AVERAGE” REPRESENTS THE MEAN PERFORMANCE RATE BETWEEN TOKEN COMPRESSION METHODS AND VANILLA LLaVA-NeXT-7B ACROSS ALL 10 BENCHMARKS. WE EVALUATE THE METHODS AT DECREASING RETENTION RATIOS FROM 75% TO 10%, WITH THE BEST RESULTS HIGHLIGHTED.

Method	VQAv2	GQA	VizWiz	SQA	VQA <sup>T</sup>	POPE	MME	MMB	MMBCN	MM-Vet	Average
<i>Upper Bound, 2880 Tokens</i>											
LLaVA-NeXT-7B [22]	81.8	64.2	57.6	70.1	61.3	86.5	1519.0	67.4	60.6	43.9	100.0%
<i>Ratio=75%, Retain up to 2160 Tokens</i>											
FastV [20]	81.1	62.5	55.1	<b>69.3</b>	59.7	86.3	1506.3	67.6	59.0	41.7	98.0%
SparseVLM [19]	81.1	62.6	55.2	68.5	<b>60.3</b>	73.2	1507.8	66.1	58.6	<b>41.9</b>	96.3%
FasterVLM [21]	81.1	63.7	<b>56.5</b>	68.4	59.1	87.5	1533.4	67.5	60.2	38.5	98.0%
<b>GlobalCom<sup>2</sup></b>	<b>81.3</b>	<b>63.8</b>	<b>56.5</b>	68.7	59.4	<b>87.8</b>	<b>1548.4</b>	<b>68.0</b>	<b>60.6</b>	40.6	<b>98.9%</b>
<i>Ratio=50%, Retain up to 1440 Tokens</i>											
FastV [20]	80.7	61.8	54.9	<b>69.1</b>	59.6	85.5	1490.3	67.4	58.5	<b>41.2</b>	97.3%
SparseVLM [19]	<b>80.9</b>	62.0	55.7	68.1	<b>60.0</b>	73.4	1484.9	65.7	58.9	39.9	95.5%
FasterVLM [21]	80.6	63.4	56.4	<b>69.1</b>	58.9	87.7	1533.3	67.4	<b>60.4</b>	39.6	98.2%
<b>GlobalCom<sup>2</sup></b>	80.6	<b>63.9</b>	<b>56.5</b>	68.5	59.5	<b>88.1</b>	<b>1552.9</b>	<b>67.6</b>	60.5	40.4	<b>98.7%</b>
<i>Ratio=25%, Retain up to 720 Tokens</i>											
FastV [20]	78.9	60.4	54.2	<b>69.8</b>	58.4	83.1	1477.3	65.6	57.0	<b>41.1</b>	95.8%
SparseVLM [19]	78.9	60.9	55.6	67.5	58.1	71.0	1446.1	63.8	57.0	38.0	93.1%
FasterVLM [21]	78.3	61.3	55.4	67.1	58.8	87.2	1454.6	<b>66.0</b>	<b>58.4</b>	37.8	95.6%
<b>GlobalCom<sup>2</sup></b>	<b>79.4</b>	<b>61.4</b>	<b>55.7</b>	68.1	<b>59.2</b>	<b>87.6</b>	<b>1493.5</b>	65.9	58.0	40.7	<b>96.9%</b>
<i>Ratio=10%, Retain up to 288 Tokens</i>											
FastV [20]	71.9	55.9	53.1	<b>69.3</b>	55.7	71.7	1282.9	61.6	51.9	33.7	87.8%
SparseVLM [19]	71.6	56.1	53.2	68.6	52.0	63.2	1332.2	54.5	50.7	24.7	83.2%
FasterVLM [21]	74.0	56.9	52.6	66.5	56.5	83.6	1359.2	61.6	<b>53.5</b>	35.0	90.3%
<b>GlobalCom<sup>2</sup></b>	<b>76.7</b>	<b>57.1</b>	<b>54.6</b>	68.7	<b>57.2</b>	<b>83.8</b>	<b>1365.5</b>	<b>61.8</b>	53.4	<b>36.4</b>	<b>91.8%</b>

multiple choices, with MMBCN [36] as its Chinese counterpart. MM-Vet [37] evaluates 16 specific capabilities across six core vision-language areas including recognition, OCR, knowledge, generation, spatial awareness, and mathematics.

*b) Implementation Details:* We select LLaVA-NeXT-7B / 13B<sup>1</sup> [22] as our baseline model. LLaVA-NeXT consists of three key components: a pre-trained CLIP-ViT-L-336px [44] for vision encoding, a pre-trained Vicuna-v1.5 as the LLM backbone, and a two-layer MLP projector that bridges them. To capture high-resolution visual information, LLaVA-NeXT pre-defines a grid configuration of  $\{2 \times 2, 1 \times \{2, 3, 4\}, \{2, 3, 4\} \times 1\}$ , allowing for a maximum resolution of  $672 \times 672$ . For our GlobalCom<sup>2</sup>,  $\tau$  and  $\alpha$  are respectively set as 10 and 0.5 for most benchmark evaluations, and we analyze the impact of these hyper-parameters on performance in Figure 3. All experiments are conducted on NVIDIA A100-SXM4-80GB GPUs.

*c) Comparison Details:* We compare our GlobalCom<sup>2</sup> with three dominant baseline methods: FastV [20], SparseVLM [19], and FasterVLM [21], by compressing visual tokens to keep the retention ratio  $R$  (75%, 50%, 25%, and 10%) of the original sequence, which comprehensively demonstrates the performance of compression methods under various compression conditions.

FastV implements one-time pruning after the second layer in the LLM backbone. SparseVLM employs pre-selected text prompts to guide pruning, aiming to minimize noise in text-visual attention. FasterVLM utilizes [CLS] attention scores from the visual encoder to rerank visual tokens and retains

the top  $R$  tokens. FastV and SparseVLM apply the retention ratio  $R$  directly to the default 2880 tokens for all input images, while both FasterVLM and our GlobalCom<sup>2</sup> perform token compression after unpadding operations on crops in LLaVA-NeXT, where  $R\%$  is applied to the length of unpadding visual token sequences. Consequently, in most cases, FasterVLM and our GlobalCom<sup>2</sup> preserve fewer visual tokens.

## B. Main Results

In this subsection, we compare our GlobalCom<sup>2</sup> with different training-free MLLM token compression methods under various retention ratios with LLaVA-NeXT-7B/13B models to evaluate their performance.

*a) Comparisons on LLaVA-NeXT-7B:* Table II presents the performance comparison of FastV [20], SparseVLM [19], FasterVLM [21], and our GlobalCom<sup>2</sup> across 10 benchmarks using LLaVA-NeXT-7B under various retention ratios. The results reveal several key findings:

- 1) Our GlobalCom<sup>2</sup> achieves superior performance across most benchmarks under various retention ratios, consistently maintaining **above 90%** of the original LLaVA-NeXT performance on average. Notably, GlobalCom<sup>2</sup> even surpasses the original LLaVA-NeXT-7B on several benchmarks. For instance, with 50% visual token retention, GlobalCom<sup>2</sup> outperforms the original LLaVA-NeXT-7B on MMB, MME, and POPE. This indicates that our GlobalCom<sup>2</sup> effectively preserves semantically rich tokens crucial for visual understanding, enabling the LLM to better comprehend and respond to image content with a few visual tokens.

<sup>1</sup>7B: <https://huggingface.co/liuhaotian/llava-v1.6-vicuna-7b>, 13B: <https://huggingface.co/liuhaotian/llava-v1.6-vicuna-13b>.

TABLE III  
COMPARISON WITH OTHER TRAINING-FREE MLLM TOKEN COMPRESSION METHODS WITH LLaVA-NeXT-13B ACROSS 10 BENCHMARKS.

Method	VQAv2	GQA	VizWiz	SQA	VQA <sup>T</sup>	POPE	MME	MMB	MMBCN	MM-Vet	Average
<i>Upper Bound, 2880 Tokens</i>											
LLaVA-NeXT-13B [22]	82.8	65.4	60.5	73.5	64.3	86.2	1575.9	70.0	64.2	48.4	100.0%
<i>Ratio=75%, Retain up to 2160 Tokens</i>											
FasterVLM [21]	<b>81.9</b>	64.6	<b>58.7</b>	72.6	62.8	87.6	1560.3	<b>69.8</b>	<b>64.8</b>	47.5	99.1%
<b>GlobalCom<sup>2</sup></b>	<b>81.9</b>	<b>65.0</b>	58.6	<b>72.8</b>	<b>62.9</b>	<b>87.8</b>	<b>1567.9</b>	69.2	64.7	<b>49.6</b>	<b>99.5%</b>
<i>Ratio=50%, Retain up to 1440 Tokens</i>											
FasterVLM [21]	<b>81.3</b>	64.2	57.0	72.5	62.4	87.6	1534.1	<b>69.5</b>	<b>64.1</b>	44.7	97.7%
<b>GlobalCom<sup>2</sup></b>	81.0	<b>64.7</b>	<b>57.1</b>	<b>73.2</b>	<b>62.5</b>	<b>87.7</b>	<b>1553.5</b>	69.3	63.5	<b>48.0</b>	<b>98.5%</b>
<i>Ratio=25%, Retain up to 720 Tokens</i>											
FasterVLM [21]	78.9	62.3	55.0	72.1	61.2	86.1	1516.1	67.6	62.1	<b>44.6</b>	95.6%
<b>GlobalCom<sup>2</sup></b>	<b>79.9</b>	<b>62.7</b>	<b>55.1</b>	<b>72.3</b>	<b>61.5</b>	<b>86.5</b>	<b>1531.2</b>	<b>67.9</b>	<b>62.2</b>	43.5	<b>95.9%</b>
<i>Ratio=10%, Retain up to 288 Tokens</i>											
FasterVLM [21]	74.5	58.1	<b>52.8</b>	70.5	58.0	81.6	1386.2	61.7	53.5	<b>38.3</b>	88.5%
<b>GlobalCom<sup>2</sup></b>	<b>77.0</b>	<b>58.3</b>	52.5	<b>71.8</b>	<b>59.1</b>	<b>82.4</b>	<b>1399.5</b>	<b>65.0</b>	<b>58.5</b>	36.2	<b>90.2%</b>

- 2) Our GlobalCom<sup>2</sup> demonstrates particularly strong performance at **low retention ratios** (e.g., 25% and 10%). Specifically, at 10% retention, we significantly outperform FastV and SparseVLM by 4.0% and 8.6% on average, highlighting our method’s effectiveness under lower visual token retention ratios. Moreover, at 10% retention, our method maintains stable performance on the visual text understanding benchmark VQA<sup>T</sup> [41], while other methods show substantial degradation (e.g., SparseVLM drops by 9.3% compared to uncompressed), demonstrating the superiority of GlobalCom<sup>2</sup> in high-resolution MLLMs token compression.
- 3) Our GlobalCom<sup>2</sup> demonstrates **significantly reduced hallucination**, particularly excelling in multi-modal hallucination evaluation on POPE [42], where it significantly outperforms baseline models and even surpasses the uncompressed LLaVA-NeXT at 75%-25% retention ratios. This indicates that equipped with our GlobalCom<sup>2</sup>, LLaVA-NeXT can effectively preserve semantically rich visual tokens, enabling better object detection in images. Furthermore, we can observe that SparseVLM, which relies on text-guided visual token compression, consistently exhibits multi-modal hallucination across various retention ratios. In contrast, vision-semantic based methods like FasterVLM and our GlobalCom<sup>2</sup> demonstrate better hallucination resistance, suggesting that text-guided approaches may overly depend on textual input while neglecting crucial visual information.

b) *Comparisons on LLaVA-NeXT-13B*: Given that FasterVLM outperforms FastV and SparseVLM in Table II significantly, and due to the unavailability of FastV and SparseVLM results on LLaVA-NeXT-13B, Table III focuses on comparing our GlobalCom<sup>2</sup> with FasterVLM. The comparison results in Table III highlights several observations:

- 1) Across 10 evaluation benchmarks, our GlobalCom<sup>2</sup> outperforms FasterVLM on most benchmarks and demonstrates superior overall average accuracy. Notably, GlobalCom<sup>2</sup> maintains **above 90%** of the uncompressed performance across various retention ratios on

both LLaVA-NeXT-7B and LLaVA-NeXT-13B models, demonstrating its effectiveness and generalizability.

- 2) At low retention ratios, our GlobalCom<sup>2</sup> demonstrates superior performance compared to FasterVLM on both the multi-modal hallucination evaluation benchmark POPE [42] and the visual text understanding benchmark VQA<sup>T</sup> [41]. Particularly, at an extremely low retention ratio of 10%, our GlobalCom<sup>2</sup> surpasses FasterVLM by 1.8% and 1.1% on POPE and VQA<sup>T</sup> [41] respectively. This superiority can be attributed to our specialized design for high-resolution MLLM token compression, which effectively preserves crucial object and textual information even at low retention rates, facilitating LLM’s comprehension of objects and text within images.
- 3) For general visual understanding benchmarks such as VQAv2 [38], MMB [36], and MMBCN [36], our GlobalCom<sup>2</sup> shows slightly lower performance than FasterVLM at high retention ratios (i.e., 75% and 50%). This is because these benchmarks emphasize overall visual information, and FasterVLM’s design ensures equal token retention across local crops, benefiting holistic image understanding. However, as the retention ratio decreases, our GlobalCom<sup>2</sup> demonstrates notably better degradation resistance compared to FasterVLM. For instance, when retention ratios drop from 25% to 10%, FasterVLM’s performance decreases by 5.9% and 8.6% on MMB and MMBCN respectively. In contrast, our GlobalCom<sup>2</sup> only drops by 2.9% and 3.7%. This advantage stems from our global thumbnail-guided semantic strategy which assists to preserve more critical visual tokens in local crops at low retention ratios.

In summary, our GlobalCom<sup>2</sup> achieves superior performance across 10 benchmarks on both LLaVA-NeXT-7B and 13B models. Notably, even under low retention ratios, our method maintains robust performance without significant degradation compared to other training-free MLLM token compression approaches. These results demonstrate that our GlobalCom<sup>2</sup> provides optimal token compression for high-resolution MLLMs.

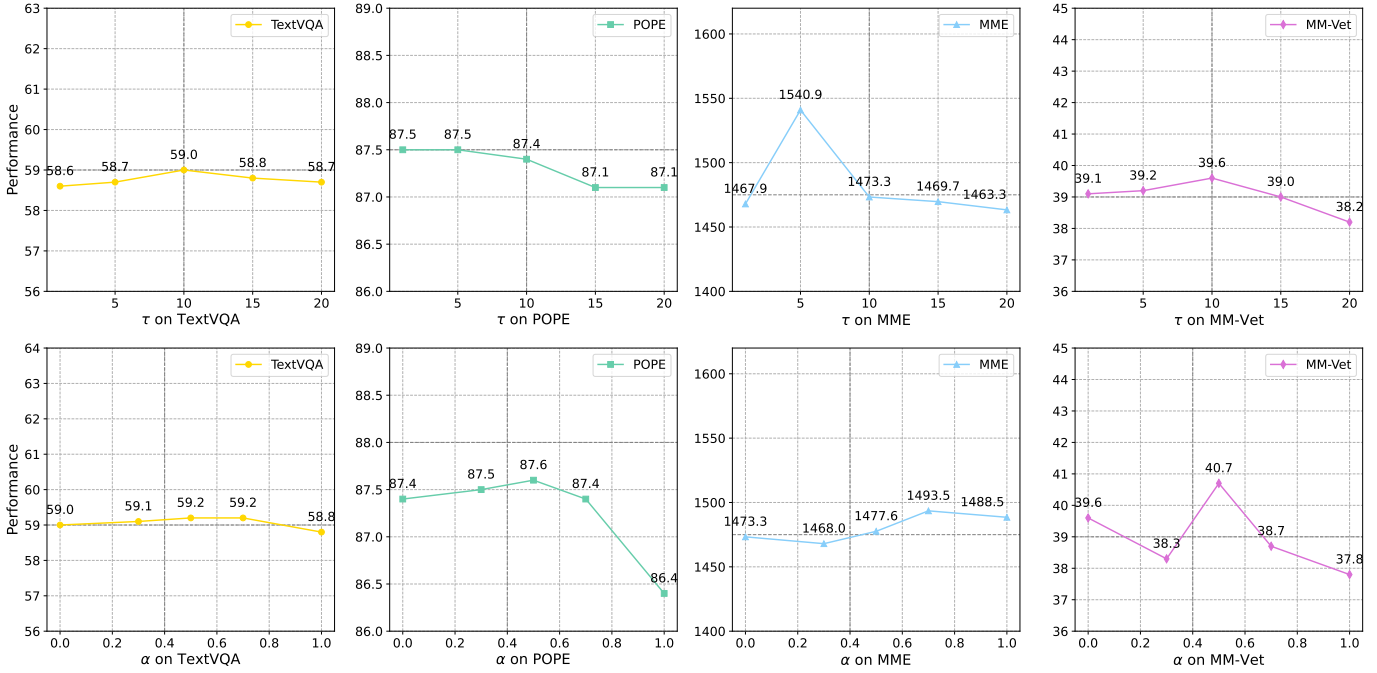


Fig. 3. **Hyper-parameter sensitivity analysis of  $\tau$  and  $\alpha$ .**  $\tau$  controls the sharpness of probability distribution in softmax when assessing local crop significance, while  $\alpha$  determines the token retention threshold where higher values indicate stronger reliance on global guidance.

TABLE IV  
ABLATION OF SIGNIFICANCE CRITERIA OF LOCAL CROPS.

Method	VQA <sup>T</sup>	POPE	MME	MM-Vet	Average
<i>Upper Bound, 2880 Tokens</i>					
LLaVA-NeXT-7B	61.3	86.5	1519.0	43.9	100.0%
<i>Ratio=25%, Retain up to 720 Tokens</i>					
Uniform	58.8	87.2	1454.6	37.8	94.6%
$n_{\text{top-}k}$	58.6	87.3	1471.5	35.7	93.7%
Softmax (max)	58.9	87.2	1462.6	38.4	95.2%
<b>Softmax (sum)</b>	<b>59.0</b>	<b>87.4</b>	<b>1473.3</b>	<b>39.6</b>	<b>96.1%</b>

TABLE V  
ABLATION OF TOKEN RETENTION CRITERIA OF LOCAL CROPS.

Method	VQA <sup>T</sup>	POPE	MME	MM-Vet	Average
<i>Upper Bound, 2880 Tokens</i>					
LLaVA-NeXT-7B	61.3	86.5	1519.0	43.9	100.0%
<i>Ratio=25%, Retain up to 720 Tokens</i>					
Local only	59.0	87.4	1473.3	39.6	96.1%
Global only	58.8	86.4	1488.5	37.8	95.0%
<b>Global and Local</b>	<b>59.2</b>	<b>87.6</b>	<b>1493.5</b>	<b>40.7</b>	<b>96.9%</b>

### C. Ablation Study and Analysis

In this sub-section, we conduct comprehensive ablation studies on our GlobalCom<sup>2</sup> under the 25% retention ratio across four representative benchmarks: VQA<sup>T</sup> [41] for visual-text understanding, POPE [42] for multi-modal hallucination evaluation, and two general instruction-following benchmarks - MME [43] and MM-Vet [37].

a) *Ablation on Retention Ratio Allocation for Local Crops:* Table IV shows the impact of different retention ratio allocation strategies for local crops. We adopt four different strategies:

- **Uniform:** Each local crop uniformly adopts a 25% retention ratio.
- $n_{\text{top-}k}$ : The retention ratio for each crop is determined by the proportion of top- $k$  tokens in its corresponding global thumbnail region to the total number of top- $k$  tokens, where  $k = 25\% \times N$  and  $N$  is the token length of global thumbnail.
- **Softmax (max):** The retention ratio for each crop is calculated as the proportion of the maximum  $s_j^G$  in its corresponding global thumbnail region to the overall  $s_j^G$ .
- **Softmax (sum):** The retention ratio for each crop is calculated as the proportion of the sum of all  $s_j^G$  in its

corresponding global thumbnail region to the overall  $s_j^G$ , which is the strategy we adopt.

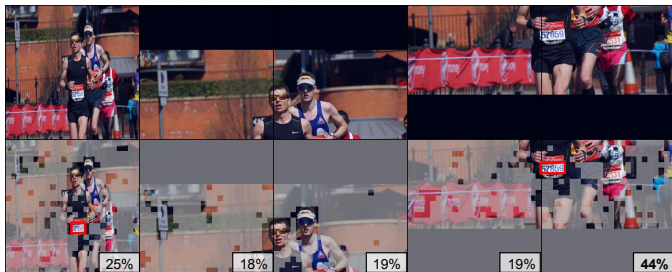
As shown in Table IV, our adopted Softmax (sum) strategy achieves the best performance, maintaining 96.1% performance of the vanilla LLaVA-NeXT-7B. Despite "Uniform", the other strategies acknowledge varying importance across local crops. However, both  $n_{\text{top-}k}$  and Softmax(max) strategies only consider the strongest visual representation capability within each local crop, rather than evaluating the overall importance of the entire local crop to the global image. In contrast, our adopted Softmax (sum) strategy adaptively allocates retention ratios based on each local crop's importance to the global image, thereby preserving more semantically visual information from high-resolution images and enabling LLM to better capture fine-grained visual signals.

b) *Ablation on Token Importance Evaluation for Local Crops:* Table V further examines the impact of different local crop token retention strategies on LLaVA-NeXT token compression, where "Global" and "Local" refer to token importance consideration at global and local levels, respectively. We observe that considering only global importance yields lower performance than considering only local importance.

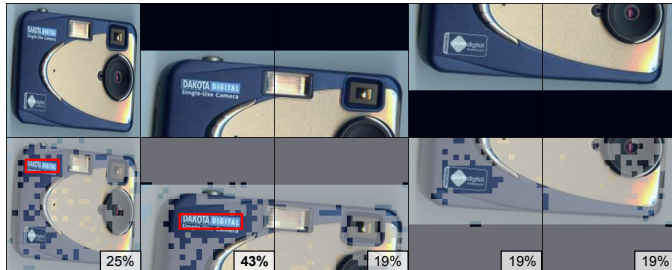
Q1: "What football league is the jacket from on the man pointing?"  
A1: "Ryman"



Q3: "What is the number of the runner in the lead right now?"  
A3: "57859"



Q2: "What is the brand of this camera?"  
A2: "DAKOTA DIGITAL"



Q4: "What time is on the clock?"  
A4: "15:08:25"

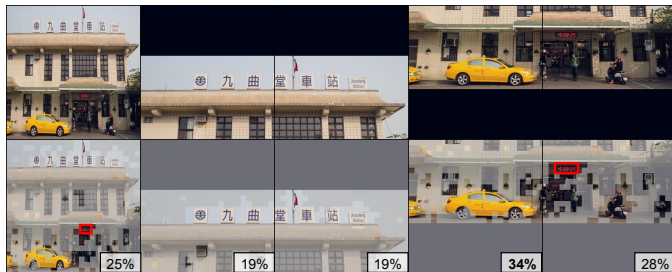


Fig. 4. Visualization of token compression by GlobalCom<sup>2</sup>. The presented examples are from VQA<sup>T</sup>, where grey masks indicate discarded visual tokens.

TABLE VI  
EFFICIENCY ANALYSIS OF OUR GLOBALCOM<sup>2</sup> WITH LLaVA-NEXT-7B ON ONE NVIDIA A100-SXM4-80GB GPU.

Method	TFLOPs↓	Total Memory (GB)↓	KV-Cache (MB)↓	Prefill Time (ms)↓	Total Time (Min & Sec)↓	Performance↑
<i>Upper Bound, 2880 Tokens</i>						
LLaVA-NeXT-7B	41.7	107.0	1536.0	170.7	15:35	1519.0
<i>Ratio=75%, Retain up to 2160 Tokens</i>						
GlobalCom <sup>2</sup>	30.4 (↓27%)	70.7 (↓34%)	1126.4 (↓27%)	119.9 (↓30%)	12:17 (↓21%)	1548.4
<i>Ratio=50%, Retain up to 1440 Tokens</i>						
GlobalCom <sup>2</sup>	19.7 (↓53%)	43.1 (↓60%)	755.0 (↓51%)	74.5 (↓57%)	9:21 (↓40%)	1552.9
<i>Ratio=25%, Retain up to 720 Tokens</i>						
GlobalCom <sup>2</sup>	9.6 (↓77%)	23.9 (↓78%)	377.0 (↓76%)	34.6 (↓80%)	7:27 (↓52%)	1493.5
<i>Ratio=10%, Retain up to 288 Tokens</i>						
GlobalCom <sup>2</sup>	3.8 (↓91%)	16.5 (↓85%)	151.0 (↓90%)	13.3 (↓92%)	5:48 (↓63%)	1365.5

TABLE VII  
EFFICIENCY ANALYSIS OF OUR GLOBALCOM<sup>2</sup> WITH LLaVA-NEXT-13B ON ONE NVIDIA A100-SXM4-80GB GPU.

Method	TFLOPs↓	Total Memory (GB)↓	KV-Cache (MB)↓	Prefill Time (ms)↓	Total Time (Min & Sec)↓	Performance↑
<i>Upper Bound, 2880 Tokens</i>						
LLaVA-NeXT-13B	80.0	172.0	2457.6	295.1	20:39	1575.9
<i>Ratio=75%, Retain up to 2160 Tokens</i>						
GlobalCom <sup>2</sup>	58.7 (↓27%)	116.0 (↓33%)	1843.2 (↓25%)	211.6 (↓28%)	16:30 (↓20%)	1567.9
<i>Ratio=50%, Retain up to 1440 Tokens</i>						
GlobalCom <sup>2</sup>	38.3 (↓52%)	72.4 (↓58%)	1228.8 (↓50%)	134.6 (↓54%)	12:49 (↓38%)	1553.5
<i>Ratio=25%, Retain up to 720 Tokens</i>						
GlobalCom <sup>2</sup>	18.7 (↓77%)	42.4 (↓75%)	590.0 (↓76%)	64.1 (↓78%)	8:48 (↓57%)	1531.2
<i>Ratio=10%, Retain up to 288 Tokens</i>						
GlobalCom <sup>2</sup>	7.4 (↓91%)	30.8 (↓82%)	236.0 (↓90%)	25.0 (↓92%)	6:53 (↓67%)	1399.5

This is because the global-only approach overlooks important fine-grained visual details in local regions, leading to degraded performance on tasks that rely heavily on visual details, such as the text recognition benchmark VQA<sup>T</sup>. Our GlobalCom<sup>2</sup> achieves optimal performance by jointly considering token importance at both global image and local crop levels.

c) *Sensitivity Analysis of Hyper-parameters:* We further explore the hyper-parameter configurations  $\tau$  and  $\alpha$  of our GlobalCom<sup>2</sup> in Figure 3.

Hyper-parameter  $\tau$  serves as the temperature in the softmax function when assessing local crop significance, controlling the “sharpness” of probability distribution. A smaller  $\tau$  leads to a

sharper distribution, amplifying the differences in global visual importance among local crops. As shown in the first row of Figure 3, our GlobalCom<sup>2</sup> demonstrates robust performance across most benchmarks, particularly on VQA<sup>T</sup> [41] and POPE [42], with varying  $\tau$  validating our design principle for high-resolution MLLMs of allocating retention ratios based on each local crop’s global importance. We empirically set  $\tau = 10$  to achieve optimal performance across most benchmarks.

Hyper-parameter  $\alpha$  determines the criterion for token retention in local crops, where a larger  $\alpha$  indicates stronger dependence on global guidance for token retention in local crops. Similar to  $\tau$ , the second row of Figure 3 shows that

our GlobalCom<sup>2</sup> exhibits consistent effectiveness across most benchmarks under different  $\alpha$  settings, substantiating our dual-perspective token retention strategy of local crops by considering their significance at both global and local levels for high-resolution MLLMs.

*d) Efficiency Analysis:* We conduct a comprehensive analysis of both theoretical and practical efficiency of our GlobalCom<sup>2</sup> with LLaVA-NeXT-7B/13B on a single NVIDIA A100-SXM4-80GB GPU, as shown in Table VI and Table VII. For theoretical efficiency, metrics except "TFLOPs" and "Total Time" are estimated using LLM-Viewer [45]. Given that the sequence length of visual tokens substantially exceeds that of textual and system tokens, we exclude the latter two from our analysis. For practical efficiency, "Total Time" and the corresponding "Performance" measurements are conducted on the MME benchmark [43].

As demonstrated in Table VI and Table VII, our GlobalCom<sup>2</sup> significantly enhances the computational efficiency of LLaVA-NeXT models in both theoretical and practical aspects. While maintaining comparable model performance, it substantially reduces GPU memory utilization and considerably accelerates inference speed. Specifically, our GlobalCom<sup>2</sup> achieves remarkable efficiency improvements: reducing computational overhead by nearly 91%, GPU memory usage by approximately 84%, KV-Cache storage by around 90%, prefill time by around 92%, and inference time by around 65%, while maintaining over 90% of the original performance by LLaVA-NeXT. Notably, these efficiency gains are accomplished without any additional re-training, highlighting the practical utility of our GlobalCom<sup>2</sup>.

#### D. Visualizations

To evaluate the effectiveness of global guidance in GlobalCom<sup>2</sup> for both global thumbnail and local crop token compression, we present token compression visualizations with a retention ratio of  $R = 25\%$  on the VQA<sup>T</sup> benchmark, which effectively measures the compression performance in high-resolution MLLMs, as shown in Figure 4.

It is clear that our GlobalCom<sup>2</sup> effectively removes redundant regions in both global thumbnails and local crops, demonstrating its ability to preserve entity-rich image regions and provide semantically meaningful visual signals to LLMs. When certain local crops exhibit significant visual redundancy within a complete image (as shown in the top-right case where the last crop largely consists of a camera's golden casing), GlobalCom<sup>2</sup> effectively assigns lower retention ratios (*i.e.*,  $r_4 = 19\%$ ) to these semantically sparse crops to eliminate redundant regions. Conversely, for crops with rich semantic content (such as the text-heavy first crop in the top-right case), GlobalCom<sup>2</sup> allocates higher retention ratios (*i.e.*,  $r_1 = 43\%$ ) to preserve these crucial visual tokens for detailed understanding.

Across all four cases, our GlobalCom<sup>2</sup> demonstrates adaptive redundancy removal across local crops while effectively preserving regions that are significant both locally and globally, enabling LLMs to capture essential information through the retained visual signals.

## V. CONCLUSION

Token compression has achieved significant progress in accelerating MLLM inference by reducing the number of visual tokens. However, existing methods have not been specifically designed for the AnyRes strategy employed by high-resolution MLLMs, leading to the discarding of important details during token compression. In this study, we propose GlobalCom<sup>2</sup>, an innovative token compression method for high-resolution MLLMs that operates on a "global-to-local" principle. The global information extracted from the thumbnail sequentially guides the selection of compression ratios for each crop and the internal token compression process, thereby adaptively preserving more critical local details. Extensive experiments across 10 multimodal benchmarks demonstrate that GlobalCom<sup>2</sup> maintains over 90% of original performance even preserving only 10% of visual tokens, which significantly outperforms existing baselines. We hope that our work can inspire future research on the acceleration of advanced MLLMs.

## REFERENCES

- [1] H. Touvron, T. Lavril, G. Izacard, X. Martinet, M. Lachaux, T. Lacroix, B. Rozière, N. Goyal, E. Hambro, F. Azhar, A. Rodriguez, A. Joulin, E. Grave, and G. Lample, "LLaMA: Open and efficient foundation language models," *arXiv preprint arXiv:2302.13971*, 2023.
- [2] OpenAI, "GPT-4 technical report," *arXiv preprint arXiv:2303.08774*, 2023.
- [3] J. Bai, S. Bai, Y. Chu, Z. Cui, K. Dang, X. Deng, Y. Fan, W. Ge, Y. Han, F. Huang, B. Hui, L. Ji, M. Li, J. Lin, R. Lin, D. Liu, G. Liu, C. Lu, K. Lu, J. Ma, R. Men, X. Ren, X. Ren, C. Tan, S. Tan, J. Tu, P. Wang, S. Wang, W. Wang, S. Wu, B. Xu, J. Xu, A. Yang, H. Yang, J. Yang, S. Yang, Y. Yao, B. Yu, H. Yuan, Z. Yuan, J. Zhang, X. Zhang, Y. Zhang, Z. Zhang, C. Zhou, J. Zhou, X. Zhou, and T. Zhu, "Qwen technical report," *arXiv preprint arXiv:2309.16609*, 2023.
- [4] H. Liu, C. Li, Q. Wu, and Y. J. Lee, "Visual instruction tuning," in *Proceedings of the Advances in Neural Information Processing Systems*, 2023.
- [5] H. Liu, C. Li, Y. Li, and Y. J. Lee, "Improved baselines with visual instruction tuning," in *Proceedings of the IEEE/CVF Conference on Computer Vision and Pattern Recognition*, 2024, pp. 26 286–26 296.
- [6] J. Bai, S. Bai, S. Yang, S. Wang, S. Tan, P. Wang, J. Lin, C. Zhou, and J. Zhou, "Qwen-VL: A frontier large vision-language model with versatile abilities," *arXiv preprint arXiv:2308.12966*, 2023.
- [7] H. Zhang, X. Li, and L. Bing, "Video-LLaMA: An instruction-tuned audio-visual language model for video understanding," in *Proceedings of the Conference on Empirical Methods in Natural Language Processing*, 2023, pp. 543–553.
- [8] Y. Bi, H. Jiang, Y. Hu, Y. Sun, and B. Yin, "See and learn more: Dense caption-aware representation for visual question answering," *IEEE Transactions on Circuits and Systems for Video Technology*, vol. 34, no. 2, pp. 1135–1146, 2024.
- [9] H. Zhang, P. Zeng, L. Gao, X. Lyu, J. Song, and H. T. Shen, "SPT: spatial pyramid transformer for image captioning," *IEEE Transactions on Circuits and Systems for Video Technology*, vol. 34, no. 6, pp. 4829–4842, 2024.
- [10] H. Qiu, L. Wang, T. Zhao, F. Meng, Q. Wu, and H. Li, "MCCE-REC: MLLM-driven cross-modal contrastive entropy model for zero-shot referring expression comprehension," *IEEE Transactions on Circuits and Systems for Video Technology*, 2024.
- [11] J. Zhu, H. Wang, and M. Shi, "Multi-modal large language model enhanced pseudo 3d perception framework for visual commonsense reasoning," *IEEE Transactions on Circuits and Systems for Video Technology*, vol. 34, no. 11, pp. 11 682–11 694, 2024.
- [12] W. Zhang, Y. Guo, J. Wang, J. Zhu, and H. Zeng, "Collaborative knowledge distillation," *IEEE Transactions on Circuits and Systems for Video Technology*, vol. 34, no. 8, pp. 7601–7613, 2024.
- [13] T. Chu, Z. Yang, and X. Huang, "Improving the post-training neural network quantization by prepositive feature quantization," *IEEE Transactions on Circuits and Systems for Video Technology*, vol. 34, no. 4, pp. 3056–3060, 2024.

- [14] J. Cha, W. Kang, J. Mun, and B. Roh, "Honeybee: Locality-enhanced projector for multimodal LLM," in *Proceedings of the IEEE/CVF Conference on Computer Vision and Pattern Recognition*, 2024, pp. 13 817–13 827.
- [15] X. Ye, Y. Gan, X. Huang, Y. Ge, Y. Shan, and Y. Tang, "VoCo-LLaMA: Towards vision compression with large language models," *arXiv preprint arXiv:2406.12275*, 2024.
- [16] Y. Shang, M. Cai, B. Xu, Y. J. Lee, and Y. Yan, "LLaVA-PruMerge: Adaptive token reduction for efficient large multimodal models," *arXiv preprint arXiv:2403.15388*, 2024.
- [17] T. Liu, L. Shi, R. Hong, Y. Hu, Q. Yin, and L. Zhang, "Multi-stage vision token dropping: Towards efficient multimodal large language model," *arXiv preprint arXiv:2411.10803*, 2024.
- [18] Y. Han, X. Liu, P. Ding, D. Wang, H. Chen, Q. Yan, and S. Huang, "Rethinking token reduction in mllms: Towards a unified paradigm for training-free acceleration," *arXiv preprint arXiv:2411.17686*, 2024.
- [19] Y. Zhang, C.-K. Fan, J. Ma, W. Zheng, T. Huang, K. Cheng, D. Gudovskiy, T. Okuno, Y. Nakata, K. Keutzer, and S. Zhang, "SparseVLM: Visual token sparsification for efficient vision-language model inference," *arXiv preprint arXiv:2410.04417*, 2024.
- [20] L. Chen, H. Zhao, T. Liu, S. Bai, J. Lin, C. Zhou, and B. Chang, "An image is worth 1/2 tokens after layer 2: Plug-and-play inference acceleration for large vision-language models," in *Proceedings of the European Conference on Computer Vision*, 2024.
- [21] Q. Zhang, A. Cheng, M. Lu, Z. Zhuo, M. Wang, J. Cao, S. Guo, Q. She, and S. Zhang, "[CLS] attention is all you need for training-free visual token pruning: Make vlm inference faster," *arXiv preprint arXiv:2412.01818*, 2024.
- [22] H. Liu, C. Li, Y. Li, B. Li, Y. Zhang, S. Shen, and Y. J. Lee, "LLaVA-NeXT: Improved reasoning, ocr, and world knowledge," 2024. [Online]. Available: <https://llava-vl.github.io/blog/2024-01-30-llava-next/>
- [23] Z. Chen, W. Wang, H. Tian, S. Ye, Z. Gao, E. Cui, W. Tong, K. Hu, J. Luo, Z. Ma, J. Ma, J. Wang, X. Dong, H. Yan, H. Guo, C. He, B. Shi, Z. Jin, C. Xu, B. Wang, X. Wei, W. Li, W. Zhang, B. Zhang, P. Cai, L. Wen, X. Yan, M. Dou, L. Lu, X. Zhu, T. Lu, D. Lin, Y. Qiao, J. Dai, and W. Wang, "How far are we to gpt-4v? closing the gap to commercial multimodal models with open-source suites," *arXiv preprint arXiv:2404.16821*, 2024.
- [24] J. Li, D. Li, S. Savarese, and S. C. H. Hoi, "BLIP-2: Bootstrapping language-image pre-training with frozen image encoders and large language models," in *Proceedings of the International Conference on Machine Learning*, 2023, pp. 19 730–19 742.
- [25] Z. Chen, J. Wu, W. Wang, W. Su, G. Chen, S. Xing, M. Zhong, Q. Zhang, X. Zhu, L. Lu, B. Li, P. Luo, T. Lu, Y. Qiao, and J. Dai, "InternVL: Scaling up vision foundation models and aligning for generic visual-linguistic tasks," in *Proceedings of the IEEE/CVF Conference on Computer Vision and Pattern Recognition*, 2024, pp. 24 185–24 198.
- [26] H. Liu, Q. You, X. Han, Y. Wang, B. Zhai, Y. Liu, Y. Tao, H. Huang, R. He, and H. Yang, "InfiMM-HD: A leap forward in high-resolution multimodal understanding," *arXiv preprint arXiv:2403.01487*, 2024.
- [27] K. Chen, R. Thapa, R. Chalamala, B. Athiwaratkun, S. L. Song, and J. Zou, "Dragonfly: Multi-resolution zoom supercharges large visual-language model," *arXiv preprint arXiv:2406.00977*, 2024.
- [28] Y. Zhang, Q. Wen, C. Fu, X. Wang, Z. Zhang, L. Wang, and R. Jin, "Beyond LLaVA-HD: Diving into high-resolution large multimodal models," *arXiv preprint arXiv:2406.08487*, 2024.
- [29] Y. Rao, W. Zhao, B. Liu, J. Lu, J. Zhou, and C. Hsieh, "DynamicViT: Efficient vision transformers with dynamic token sparsification," in *Proceedings of the Advances in Neural Information Processing Systems*, M. Ranzato, A. Beygelzimer, Y. N. Dauphin, P. Liang, and J. W. Vaughan, Eds., 2021, pp. 13 937–13 949.
- [30] X. Liu, T. Wu, and G. Guo, "Adaptive sparse vit: Towards learnable adaptive token pruning by fully exploiting self-attention," in *Proceedings of the International Joint Conference on Artificial Intelligence*, 2023, pp. 1222–1230.
- [31] Y. Liang, C. Ge, Z. Tong, Y. Song, J. Wang, and P. Xie, "Not all patches are what you need: Expediting vision transformers via token reorganizations," in *Proceedings of the International Conference on Learning Representations*, 2022.
- [32] D. Bolya, C. Fu, X. Dai, P. Zhang, C. Feichtenhofer, and J. Hoffman, "Token merging: Your ViT but faster," in *Proceedings of the International Conference on Learning Representations*, 2023.
- [33] W. Chai, E. Song, Y. Du, C. Meng, V. Madhavan, O. Bar-Tal, J. Hwang, S. Xie, and C. D. Manning, "AuroraCap: Efficient, performant video detailed captioning and a new benchmark," *arXiv preprint arXiv:2410.03051*, 2024.
- [34] A. Vaswani, N. Shazeer, N. Parmar, J. Uszkoreit, L. Jones, A. N. Gomez, Ł. Kaiser, and I. Polosukhin, "Attention is all you need," in *Proceedings of the Advances in Neural Information Processing Systems*, vol. 30, 2017, pp. 5998–6008.
- [35] P. Lu, S. Mishra, T. Xia, L. Qiu, K. Chang, S. Zhu, O. Tafjord, P. Clark, and A. Kalyan, "Learn to explain: Multimodal reasoning via thought chains for science question answering," in *Proceedings of the Advances in Neural Information Processing Systems*, 2022, pp. 2507–2521.
- [36] Y. Liu, H. Duan, Y. Zhang, B. Li, S. Zhang, W. Zhao, Y. Yuan, J. Wang, C. He, Z. Liu, K. Chen, and D. Lin, "MMBench: Is your multi-modal model an all-around player?" in *Proceedings of the European Conference on Computer Vision*, 2024, pp. 216–233.
- [37] W. Yu, Z. Yang, L. Li, J. Wang, K. Lin, Z. Liu, X. Wang, and L. Wang, "MM-Vet: Evaluating large multimodal models for integrated capabilities," in *Proceedings of the International Conference on Machine Learning*, 2024.
- [38] Y. Goyal, T. Khot, D. Summers-Stay, D. Batra, and D. Parikh, "Making the V in VQA matter: Elevating the role of image understanding in visual question answering," in *Proceedings of the IEEE/CVF Conference on Computer Vision and Pattern Recognition*, 2017, pp. 6325–6334.
- [39] D. A. Hudson and C. D. Manning, "GQA: A new dataset for real-world visual reasoning and compositional question answering," in *Proceedings of the IEEE/CVF Conference on Computer Vision and Pattern Recognition*, 2019, pp. 6700–6709.
- [40] D. Gurari, Q. Li, A. J. Stangl, A. Guo, C. Lin, K. Grauman, J. Luo, and J. P. Bigham, "VizWiz grand challenge: Answering visual questions from blind people," in *Proceedings of the IEEE/CVF Conference on Computer Vision and Pattern Recognition*, 2018, pp. 3608–3617.
- [41] A. Singh, V. Natarajan, M. Shah, Y. Jiang, X. Chen, D. Batra, D. Parikh, and M. Rohrbach, "Towards VQA models that can read," in *Proceedings of the IEEE/CVF Conference on Computer Vision and Pattern Recognition*, 2019, pp. 8317–8326.
- [42] Y. Li, Y. Du, K. Zhou, J. Wang, W. X. Zhao, and J. Wen, "Evaluating object hallucination in large vision-language models," in *Proceedings of the Conference on Empirical Methods in Natural Language Processing*, 2023, pp. 292–305.
- [43] C. Fu, P. Chen, Y. Shen, Y. Qin, M. Zhang, X. Lin, Z. Qiu, W. Lin, J. Yang, X. Zheng, K. Li, X. Sun, and R. Ji, "MME: A comprehensive evaluation benchmark for multimodal large language models," *arXiv preprint arXiv:2306.13394*, 2023.
- [44] A. Radford, J. W. Kim, C. Hallacy, A. Ramesh, G. Goh, S. Agarwal, G. Sastry, A. Askell, P. Mishkin, J. Clark, G. Krueger, and I. Sutskever, "Learning transferable visual models from natural language supervision," in *Proceedings of the International Conference on Machine Learning*, 2021, pp. 8748–8763.
- [45] Z. Yuan, Y. Shang, Y. Zhou, Z. Dong, Z. Zhou, C. Xue, B. Wu, Z. Li, Q. Gu, Y. J. Lee, Y. Yan, B. Chen, G. Sun, and K. Keutzer, "LLM inference unveiled: Survey and roofline model insights," *arXiv preprint arXiv:2402.16363*, 2024.